METHODS AND APPLICATIONS OF ANALYSIS.
Vol. 28, No. 3, pp. 355–370, September 2021

007

A FULLY COMPATIBLE STAGGERED LAGRANGIAN ALGORITHM FOR ELASTIC-PLASTIC FLOWS UTILIZING THE CONSERVATION OF TOTAL ENERGY*

YUELING JIA†‡, SONG JIANG†, AND JUN-BO CHENG†

Dedicated to Professor Ling Hsiao on the occasion of her 80th birthday

Abstract. In this paper we construct a fully compatible staggered Lagrangian algorithm for the equations of two-dimensional elastic-plastic flows (FCSLAEP), with the hypo-elastic incremental constitutive model, von Mises' yielding condition and the Mie-Grüneisen equation of state. To construct our scheme, we first reformulate all governing equations of elastic-plastic flows, including the equations of deviatoric stress, into a hyperbolic system in the form of the divergence and the gradient operators. Then, this hyperbolic system is discretized by adapting the method of support operators and using some new vector identities of differential calculus. Moreover, we replace the finite volume surface integrals with the line integrals and rewrite the equations of deviatoric stress in the form of the internal energy on the right-hand side (so that one can use the gradient operator on the velocity in the discrete form), to discretize the equations of deviatoric stress in order to conserve the total energy and preserve the symmetry. Finally, the predictor-corrector technique is used with respect to time to improve the accuracy. A number of numerical tests are carried out, and the numerical results show that the proposed scheme FCSLAEP seems robust and convergent. Moreover, the scheme is of the 2nd order accuracy, and conserves the total energy and preserves the symmetry.

Key words. 2D elastic-plastic flows, hypo-elastic constitutive model, Mie-Grüneisen equation of state, fully compatible staggered Lagrangian algorithm, conservation of total energy, preservation of symmetry.

Mathematics Subject Classification. 74C05, 74F10, 74M20, 68U05, 68U09.

1. Introduction.

This paper aims at the construction of a fully compatible staggered Lagrangian scheme for the equations of elastic-plastic flows with the hypo-elastic incremental constitutive model, which was initially developed by Wilkins [1].

The early numerical simulations for the elastic-plastic hydrodynamic equations with Wilkins' model were carried out on staggered grids, based on the Lagrangian approach[13, 14]. For the staggered Lagrangian approach, the physical variables are defined in the cell center, while the velocity and the position are defined at the cell corner. Therefore, the geometric conservation law (GCL) is satisfied [13]. However, the equations of specific internal energy and momentum are discretized in different control volumes, this makes the conservaion of total energy failed.

Driven by engineer applications, Dobrev, et al. proposed curvilinear finite element methods for both hydrodynamics and elastic-plastic Lagrangian dynamics, and further developed a multi-physics parallel arbitrary Lagrangian Eulerian (ALE) platform MARBL to simulate multi-material hydrodynamic problems [3, 4, 5, 6]. For Lagrangian hydrodynamics, a curvilinear finite element method was proposed in [7], then extended to a high-order curvilinear finite element method in [8]. In [9], a high-order curvilinear finite element method was studied for axisymmetric Lagrangian hydrodynamics, while the geometry validity of curvilinear finite elements was investigated in [10]. Furthermore, a high-order curvilinear finite element method for elastic-plastic Lagrangian dynamics was recently developed in [11] under the condition that the

*Received January 12, 2021; accepted for publication December 30, 2021.
†Institute of Applied Physics and Computational Mathematics, Beijing, 100094, China.
‡Corresponding author (Email: jia_yueling@iapcm.ac.cn).

strong mass conservation has to be satisfied in any moving volume (in order to eliminate the computation of the density from the numerical scheme), an additional condition which has to be a priori verified. In [8] an extension of the high order curvilinear finite element method to Lagrangian hydrodynamics was investigated.

In the traditional Lagrangian numerical method, both the artificial and hourglass viscosity terms are used to suppress spurious numerical oscillations and to avoid hourglass-type meshes. In [11] and [8], the so-called tensor artificial viscosity is employed in the framework of a finite element approach to compute moving shocks [12], where the authors do not employ the hourglass viscosity term due to the use of moving curvilinear meshes. Besides the staggered Lagrangian/ALE schemes, the Eulerian and cell-centered Lagrangian schemes [13, 14] have also been proposed for elastic-plastic flows. Maire et al. [13] developed a second-order cell-centered scheme by constructing a node-solver. Cheng et al. proposed a compatible cell-centered scheme within the framework of the Godunov method which is shown to satisfy GCL [14].

As mentioned at the beginning of this paper, we shall develop a fully compatible staggered Lagrangian algorithm for elastic-plastic flows with Wilkins' hypo-elastic incremental constitutive model.

This paper focus on compatible staggered Lagrangian methods where equations of momentum and specific internal energy are discretized on different grid. The artificial viscosity is employed to simulate moving shocks in order to damp spurious numerical oscillations. Furthermore, the hourglass viscosity is needed in the straight line grid to resist hourglass-type grid appear. The viscosity appears in the total stress matrix as a force and is taken as part of the corner force.

The compatible staggered Lagrangian hydrodynamics algorithm (CSLHA) for fluid flows was initially introduced by Caramana et al. in [15], where the equations of hydrodynamic flows are formulated in the form of the gradient and divergence operators, and discretized as a whole system by applying the method of support operators. In [16] Barlow et al. applied CSLHA to the constrained optimization framework for interface-aware sub-scale closure models for multi-material cells in Lagrangian and ALE hydrodynamics. CSLHA was also applied to the equations of elastic-plastic flows with the generic difference of deviatoric stress in [17, 18], where the constructed algorithms are unfortunately compatible with the hypo-elastic constitutive model, that means, the constructed algorithm do not rigorously satisfy the conservation of total energy.

In this paper, based on the method of support operators, we shall construct a fully compatible staggered Lagrangian algorithm for elastic-plastic flows which should satisfy the conservation of total energy and other physical laws such as Newton's second and third laws(in the discrete form), and preserve the symmetry of solutions. Therefore, we shall treat all the continuum equations, inclusive of the hypo-elastic constitutive model, as a whole system in order to make our discretization satisfy the physical laws, such as the conservation of total energy and Newton's third law, etc. For elastic-plastic flows, the hypo-elastic constitutive model [1], which models the equations of the deviatoric stress, is independent of three balance laws, but should be compatibly discretized as the other equations in the whole system in order to conserve the total energy and the other physical properties. This makes the conserved discretization of the total energy in a staggered Lagrangian algorithm for elastic-plastic flows more challenging than that for hydrodynamic flows from [15]. For elastic-plastic flows, the divergence operator acts both on the velocity field and on the stress tensor, while the gradient operator acts on the velocity field. This makes the construction of a

compatible discretization algorithm more complex than that for hydrodynamic flows for which the gradient operator acts on the pressure and the divergence operator on the velocity only. Moreover, the equations of deviatoric stress for elastic-plastic flows are complicated and special treatments are needed.

Roughly speaking, the basic idea of our algorithm is that we can fortunately reformulate all the equations of elastic-plastic flows, particularly together with the hypo-elastic incremental constitutive model [1], as a whole system of the divergence and gradient operators. Then, we can adapt the method of support operators to compatibly discretize the full system. Therefore, we call our algorithm the full compatible staggered Lagrangian algorithm for elastic-plastic flows (FCSLAEP).

We should address here that exploiting *the identity of operators*:

$$\nabla \cdot (\sigma \cdot \vec{v}) = \sigma : (\nabla \vec{v}) + \vec{v} \cdot (\nabla \cdot \sigma)\,, \tag{1}$$

and using the definition of the divergence operator on the velocity field, we first discretize the divergence operator on the stress tensor. Then, the discretized gradient operator on the velocity field can be derived from the conservation of total energy and the identity of operators (1). Consequently, the conservation of total energy is satisfied in a natural and compatible way.

This paper is organized as follows. In Section 2, the governing equations of elastic-plastic flows with Wilkins' hypo-elastic model are given in the two-dimensional planar geometry, and fully transformed in the form of the gradient and divergence operators, which is convenient to discrete via the method of support operators. In Section 3 we construct a fully compatible Lagrangian algorithm, while in Section 5 we employ the predictor-corrector technique to finally give the proposed scheme FCSLAEP of this paper. Section 5 presents some numerical tests to validate FCSLAEP. The conclusions are given in Section 6.

2. Governing equations and fundamental ideas. Assume that there is a discrete volume element V that may deform in shape but through whose boundary no mass flows. This is the basic assumption of all Lagrangian algorithms, and will be called the Lagrangian assumption in what follows. Therefore, the original mass present in the volume at some starting time, M_0, is constant. At any later time, t, the density, ρ, inside the given element is simply found from $\rho = \frac{M_0}{V}$. Substituting this expression into the continuity equation for mass, we obtain the so-called geometrical conservation law:

$$\frac{1}{V}\frac{dV}{dt} = \nabla \cdot \vec{v} \equiv \frac{\partial v_r}{\partial r} + \frac{\partial v_z}{\partial z}, \tag{2}$$

where $\frac{d}{dt}$ is the material derivative, $V = 1/\rho$ and $\vec{v} = (v_r, v_z)$.

Now, we consider the equation of motion with the force given as the gradient of the stress tensor σ, and also, the associated equation for the internal energy e, together with the incremental constitutive law for the deviatoric stress, written in the Lagrangian form:

$$\rho\frac{d\vec{v}}{dt} = \nabla \cdot \sigma, \tag{3}$$

$$\rho\frac{de}{dt} = \sigma : (\nabla \vec{v}), \tag{4}$$

$$\frac{d\mathbf{S}}{dt} = 2\mu\mathbf{D}_0 - (\mathbf{SW} - \mathbf{WS}). \tag{5}$$

Here the inner product of $\mathbf{A}$ and $\mathbf{B}$ is defined as $\mathbf{A} : \mathbf{B} = \sum a_{ij}b_{ji}$ (i.e., $= tr(\mathbf{A^T B})$) for any pair of tensors. The stress tensor σ is decomposed into a pressure p and a deviatoric stress $\mathbf{S}$ by $\sigma = \mathbf{S} - p\mathbf{I}$, which includes the components $\sigma_{ij} = S_{ij} - p\delta_{ij}$, $\tau_{ij} = S_{ij}$; $\mathbf{D}_0 = \mathbf{D} - \frac{1}{3}tr(\mathbf{D})\mathbf{I}$ with the strain rate tensor $\mathbf{D} = \frac{1}{2}\left(\nabla\vec{v} + (\nabla\vec{v})^T\right)$, and $tr(\mathbf{D}) = \nabla \cdot \vec{v} = \frac{\partial v_r}{\partial r} + \frac{\partial v_z}{\partial z}$; $\mathbf{W} = \frac{1}{2}\left(\nabla\vec{v} - (\nabla\vec{v})^T\right)$ and μ is the shear modulus. The von Mises' yielding condition is used to describe the elastic limit. In two dimensions, it is given by $\mathbf{S} = \mathbf{S} \times \min\left(1, \sigma_y/\sqrt{\frac{3}{2}(\mathbf{S} : \mathbf{S})}\right)$, where σ_y is the yielding strength of the material in simple tension.

To complete the system (3)–(5), an equation of state of the form $p = p(\rho, e)$ has to be specified. In this paper, for the equation of state we consider the following Mie-Grüneisen model:

$$p(V, \varepsilon) = \frac{a_0^2(V_0 - V)}{[V_0 - s(V_0 - V)]^2} + \frac{\Gamma(V)}{V}\left[\varepsilon - \frac{1}{2}\left(\frac{a_0(V_0 - V)}{V_0 - s(V_0 - V)}\right)^2\right]. \tag{6}$$

The full system (3)–(5) will be discretized so that the total energy is conserved. To this end, we shall rewrite the equations of the deviatoric stress as the right-hand side of the equations for the (specific) internal energy in the form of the gradient operator. Then, we are able to discretize the full system of elastic-plastic flows in a way similar to that for the system of hydrodynamic flows in which only the divergence and gradient operators appear. Thus, applying the method of support operators, we can construct full compatible discretization of the equations of elastic-plastic flows by first defining the divergence operator discretization and then deriving the gradient operator discretization.

First, we reformulate the evolution equations of the deviatoric stress as follows.

$$\frac{d\mathbf{S}}{dt} = \mathbf{N} : (\nabla\vec{v}). \tag{7}$$

where the tensors N_{rz}, corresponding to the deviatoric stress S_{rz}, read as

$$\mathbf{N}_{rr} = \begin{pmatrix} \frac{4\mu}{3} & -s_{rz} \\ s_{rz} & -\frac{2\mu}{3} \end{pmatrix}, \mathbf{N}_{zz} = \begin{pmatrix} -\frac{2\mu}{3} & s_{rz} \\ -s_{rz} & \frac{4\mu}{3} \end{pmatrix}$$

$$\mathbf{N}_{rz} = \begin{pmatrix} 0 & \mu - \frac{s_{zz} - s_{rr}}{2} \\ \mu + \frac{s_{zz} - s_{rr}}{2} & 0 \end{pmatrix}.$$

We remark that the above tensors are not symmetrical, this brings some difficulties in the construction of a fully compatible staggered Lagrangian algorithm for elastic-plastic flows because the stress tensor is symmetric.

Next, we use the method of support operators to give the compatible staggered discretization. We give some basic concepts and notations for the staggered quadrilateral grid formulation in the following Fig. 1.

A quadrilateral z is defined by points labeled as from 1 to 4 which are connected by solid lines. The midpoint of solid lines grid is connected by the dash lines. The center point z of the quadrilateral is defined by the simple average of the coordinates of four

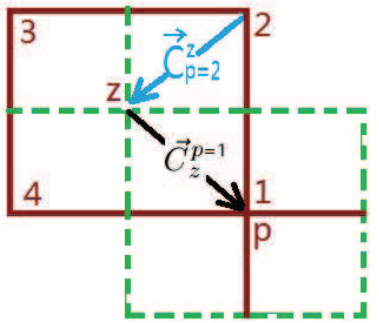

FIG. 1. *Staggered grid of solid lines with center z and four nodes p*

points denoted by p (the same as the center point of the quadrilateral which is made by the midpoints of the opposite quadrilateral sides). For simplicity, the straight lines make the "coordinate-line" mesh, while the dash lines connect the "median" meshes. These correspond to the primary and dual grids, respectively. A staggered scheme means that the velocity and position are defined at the cell point of the primary grid, while the specific internal energy, pressure, and density, the strain tensor and the deviatoric stress are constant inside of a quadrilateral cell. In general, those labels z and p are always used as subscripts or superscripts with integer values that range over all the cell points and grid corners, respectively. Therefore, $\overrightarrow{C}_z^{p=1}$ is the vector from a corner $p = 1$ to an ambient cell center z, while $\overrightarrow{C}_{p=1}^z$ is the vector from a ambient cell center z to a corner $p = 1$. Summations are always performed with respect to the lower index. Similarly, the forces $\overrightarrow{f}_z^{p=1}$ and $\overrightarrow{f}_{p=1}^z$ satisfy Newton's third law: $\overrightarrow{f}_z^{p=1} = -\overrightarrow{f}_{p=1}^z$, a key relation to make our discretization satisfy the total energy conservation. This relation is to say, the force $\overrightarrow{f}_z^{p=1}$ from the cell z acts on the corner $p = 1$, while the force $\overrightarrow{f}_{p=1}^z$ from the corner $p = 1$ acts on the cell z, both forces appear simultaneity and possess the same magnitude, but in the opposite directions.

The concept of a "corner" is the same as that in [15]. The corner volume associated with a cell point p and a cell z in two dimensions is the volume inside the surface defined through the point p, the two midpoints of the lines through points p of cell z, and the corner volumes to each quadrilateral cell. The corner mass, associated with the point p and cell z, is defined as m_p^z (which satisfies $m_p^z = m_z^p$), as the mass inside the associated corner volume at some time t. The summations are always performed with respect to the lower index. The corner mass is used as the primitive quantity from which the grid and nodal, or grid point, masses can be constructed. The total mass of point p(or z) can be obtained by summation of all corner masses of ambient cells z (or points p) around the fixed point p (or cell z) as

$$M_p = \sum_z m_z^p, \quad M_z = \sum_p m_p^z.$$

The Lagrangian assumption guarantees that M_z is a constant, However, M_p is allowed to vary with time. Both the zonal and the corner masses are considered on a totally equal footing and are constant. The grid and the nodal masses are composed of the same objects that are simply added in a different order, it follows that the

zonal and nodal masses in a problem are equal, that is to say, $\sum_z M_z = \sum_p M_p$. For the nodal mass of some boundary point in a physical region, it is always assumed that the corner masses exterior to that region are zero.

3. A fully compatible Lagrangian algorithm. In this section we give the discretization of the equations of elastic-plastic flows with the help of the method of support operators. The important feature in a staggered Lagrangian discretization is that the momentum equations evolve in time at the nodes, while the evolutionary equation of the specific internal energy is defined in the grids. Therefore, the equation for the conservation of total energy is composed of a mix of the variable definitions. This allows one to extend the Lagrangian assumption in a natural manner that eliminates under constrained modes of distortion [15], and to specify the discrete forces without additional assumptions about the manner in which the work performed at cell interfaces is to be divided into the kinetic and internal energies, as is necessary for point-centered formulations when operator prescriptions for these forces are not available. However, care must be taken with staggered grid formulations so that logical inconsistencies between quantities defined at nodes and grids do not occur.

Next, we utilize the momentum equation to introduce the important concept of a corner force by using the forces of the strain tensor. Thus, we can define the total energy on a single grid basis and extend it to the entire domain of integration. The discretizd internal energy equation can be derived in a production form of a arbitrary corner force and a zonal point velocity, which is identical to that obtained by a direct discretization of the internal energy equation for the special case of forces that arise from a strain tensor of piecewise constant in a grid.

The arbitrary corner force in the discretized internal equation can be chosen in different manners, but should be kept identical to that in the discretized momentum equations in order to preserve the conservation of total energy.

Denote the area, volume and mass of a cell z by A_z, V_z and M_z, taking the different coordinates into account. Denote by $\overrightarrow{C}_z^p$ the point-vectors associated with the accept force point p of a ambient cell z (z denotes the sum variable and p the fixed point), then $\overrightarrow{C}_z^1 = (\frac{z_4-z_2}{2} \quad \frac{r_2-r_4}{2})^T$, $\overrightarrow{C}_z^2 = (\frac{z_1-z_3}{2} \quad \frac{r_3-r_1}{2})^T$, $\overrightarrow{C}_z^3 = (\frac{z_2-z_4}{2} \quad \frac{r_4-r_2}{2})^T$, $\overrightarrow{C}_z^4 = (\frac{z_3-z_1}{2} \quad \frac{r_1-r_3}{2})^T$.

The fully staggered compatible Lagrangian algorithm for the system (3)–(5) are given by

$$M_p \frac{d\vec{v}_p}{dt} = \int_{V_p} \nabla \cdot \sigma dV = \int_{\partial V_p} \sigma d\vec{s} = \sum_z \vec{f}_z^p \equiv \vec{F}_p,$$

where $\vec{f}_z^p$ is the force that cell z acts on its point p. One should notice that $\vec{f}_z^p$ and $\vec{f}_p^z$ obey Newton's laws, such as Newton's second and third laws. So, there are four forces on a quadrilateral cell corresponding to its four nodes. As a point, there are four cells around it, which contributes to the corner force of corner p. Define the divergence of the velocity in the median mesh as follows.

$$(\nabla \cdot \vec{v})_{z=1} = \frac{1}{V_{z=1}} \sum_p \vec{v}_p \cdot \vec{C}_p^{z=1},$$

which makes the divergence of the node velocity work on the cell z. This definition is extended to the divergence of the stress tensor in coordinate-line meshes which makes

the divergence of the stress tensor in cell z work on the nodes:

$$V_p(\nabla \cdot \sigma)_p = \sum_z \vec{f}_z^p = \sum_z (\sigma_z \cdot \vec{C}_z^p).$$

The above identity is used in discretizing the momentum equation with all artificial forces, such as the artificial/hourglass viscosity, to update the acceleration, velocity and node position at the $(n+1)$-th time level. Hence, $\vec{f}_z^p$ includes the bulk artificial viscosity q, which is treated as part of the pressure when shocks arise, while the hourglass viscosity is directly added to the force $\vec{f}_z^p$.

Thus, the acceleration, velocity, node position, as well as the velocity at the $(n+\frac{1}{2})$-time level (which we call the semi-time level velocity thereafter) are given by

$$a_p^{n+1} = \tfrac{1}{M_p} \sum_z \vec{f}_z^p = \tfrac{1}{M_p} \sum_z (\sigma_z \cdot \vec{C}_z^p), \tag{8}$$

$$\vec{v}_p^{n+1} = \vec{v}_p^n + \tfrac{\Delta t}{M_p} \sum_z \vec{f}_z^p = \vec{v}_p^n + \tfrac{\Delta t}{M_p} \sum_z (\sigma_z \cdot \vec{C}_z^p), \tag{9}$$

$$\vec{v}_p^{n+\frac{1}{2}} = \frac{1}{2}\left(\vec{v}_p^n + \vec{v}_p^{n+1}\right) = \vec{v}_p^n + \tfrac{\Delta t}{2M_p} \sum_z \vec{f}_z^p = \vec{v}_p^n + \tfrac{\Delta t}{2M_p} \sum_z (\sigma_z \cdot \vec{C}_z^p). \tag{10}$$

On the other hand, based on the definition of the discretized divergence, we deduce the discretized gradient of the velocity via the conservation of total energy as follows.

$$\sigma_z : (\nabla \vec{v}) = -\frac{1}{V_z} \sum_p \left(\vec{f}_p^z\right) \cdot \vec{v}_p = -\frac{1}{V_z} \sum_p \left(\sigma_z \cdot \vec{C}_p^z\right) \cdot \vec{v}_p, \tag{11}$$

which is used in the discretization of the balance equation for the specific internal energy in the following:

$$e_z^{n+1} = e_z^n - \frac{\Delta t}{M_z^n} \sum_p \left(\sigma_z \cdot \vec{C}_p^z\right) \cdot \vec{v}_p. \tag{12}$$

The left-hand side of (11) is the inner product of the stress tensor with the velocity gradient. Fortunately, the evolutionary equations of deviatoric stress can be rewritten as the inner product of some tensor with the velocity gradient, and could be discretized similarly to the evolutionary equation of the specific internal energy as follows.

$$\mathbf{N}_{rz} : (\nabla \vec{v}) = -\frac{1}{V_z} \sum_p \left(\vec{f}_{N_{rz}}^z\right) \cdot \vec{v}_p = -\frac{1}{V_z} \sum_p \left(\mathbf{N}_{rz} \cdot \vec{C}_p^z\right) \cdot \vec{v}_p,$$

which is used in discretizing the deviatoric stresses S_{rr}^{*n+1}, S_{zz}^{*n+1}, S_{rz}^{*n+1} as follows.

$$S_{rz}^{n+1} = S_{rz}^n - \frac{\Delta t}{V_z^n} \sum_p \left(\mathbf{N}_{rz} \cdot \vec{C}_p^z\right) \cdot \vec{v}_p. \tag{13}$$

We point out here that the above discretization for the equations of deviatoric stress is based on the finite volume surface integrals, a process similar to that for the gradient operator on the right-hand side of the internal energy equation.

For Lagrangian hydrodynamic flows, it is well-known that when the momentum and internal energy equations are discretized with the line and finite volume surface integrals to preserve symmetry, respectively, such a scheme is often called "area-weighted scheme". When both the momentum and internal energy equations are discretized with the finite volume surface integrals to preserve the total energy, such a scheme is often called "volume-weighted scheme". For the equations of elastic-plastic flows considered in this paper, however, a traditional "area-weighted scheme"/"volume-weighted scheme" is not sufficient to guarantee symmetry/conservation of total energy due to the presence of the additional equations of deviatoric stress. In this paper we use the gradient operator to act on the velocity to produce a deformation tensor, which includes diliational shear, and rotational components. Consequently, the symmetry is achieved by replacing the finite volume surface integrals with the line integrals in the discretization of the equations of deviatoric stress:

$$\mathbf{S}_z^{n+1} = \mathbf{S}_z^n - \tfrac{\Delta t}{A_z^n}\mathbf{N}_{iz}^p : (\vec{v}_p^z \cdot \overrightarrow{C}_p^z). \tag{14}$$

4. A fully compatible staggered Lagrangian algorithm for elastic-plastic flows (FCSLAEP). In this section we present a second-order predictor-corrector time-integration method for the fully compatible staggered Lagrangian spatial-discretization for the equations of elastic-plastic flows.

4.1. Predictor step. The discretized momentum equation gives us the update of the node velocity and node position, and thus the semi-time level velocity from the new acceleration. Then, after the acceleration is updated, the slide lines and the rigid wall boundary should be updated, thus possibly changing the value of the semi-time level velocity, and consequently violating the conservation of total energy. To circumvent such difficulties, and to introduce the proper entropy changes due to shocks and to reduce possible spurious oscillations, we utilize the bulky artificial viscosity q_{rb} in the algorithm. The hourglass viscosity $\vec{f}_{hgs}$ is added in the discretized momentum equation as follows.

$$V_p(\nabla \cdot \sigma)_p = \sum_z \vec{f}_z^p = \sum_z (\sigma_z \cdot \vec{C}_z^p + \vec{f}_{hgs}).$$

$$\sigma_z = \begin{pmatrix} S_{rr} - (p + q_{rb}) & \tau_{rz} \\ \tau_{rz} & S_{zz} - (p + q_{rb}) \end{pmatrix}.$$

Then, the predictor step for the acceleration is given by

$$a_p^{*n+1} = \tfrac{1}{M_p^n} \sum_z (\vec{f}_z^p)^n = \tfrac{1}{M_p^n} \sum_z (\sigma_z \cdot \vec{C}_z^p + \vec{f}_{hgs})^n. \tag{15}$$

The slide lines or rigid walls are computed to correct the time step, acceleration, velocity and node position when they are involved in the problem. Then, based on the corrected node vectors at the n-th time level, the predictor step for the velocity reads as

$$\vec{v}_p^{*n+1} = \vec{v}_p^n + a_p^{*n+1}\Delta t, \tag{16}$$

$$\vec{v}_p^{*n+1/2} = \frac{1}{2}\left(\vec{v}_p^n + \vec{v}_p^{*n+1}\right) = \vec{v}_p^n + \tfrac{\Delta t}{2} a_p^{*n+1}. \tag{17}$$

By virtue of (15)–(17), the specific internal energy and the deviatoric stresses in the predictor step read as

$$e_z^{*n+1} = e_z^n - \frac{\Delta t}{M_z^n} \sum_p \left(\sigma_z \cdot \vec{C}_p^z + \vec{f}_{hgs}\right)^n \cdot \vec{v}_p^{*n+\frac{1}{2}}, \tag{18}$$

$$S_{rz}^{*n+1} = S_{rz}^n - \frac{\Delta t}{A_z^n} \sum_p \mathbf{N}_{iz}^n : (\vec{v}_p^{*n+1/2} \cdot \vec{C}_p^n). \tag{19}$$

The local speed of sound for elastic-plastic flows is given by

$$C = \frac{4\mu}{3} + \rho_0 \frac{\partial p}{\partial \rho}\bigg|_e + p\left(\frac{V}{V_0}\right)^2 \frac{\partial p}{\partial e}\bigg|_\rho.$$

Here the shear modulus also contributes to the local speed of sound which is used to obtain the time step:

$$\Delta t = c_t l \left[q + \sqrt{q^2 + C^2}\right]^{-1}, \quad q = q_1 l \left|\nabla \cdot v\right| + q_2 C,$$

where $c_t < 0.5$ is a given constant, l is the characteristic length of the cell; q_1 and q_2 are parameters. In this paper we take $q_1 = 1.5$ and $q_2 = 0.06$. The bulky artificial viscosity force is given by

$$q_{rb} := \rho_0 l \left|\nabla \cdot \vec{v}\right| \left(q_2 C + q_1 l \left|\nabla \cdot \vec{v}\right|\right).$$

For resisting the hourglass distortion of the grid, the hourglass viscosity force is given below

$$\vec{f}_i = (-1)^i a \left(\vec{v}_1 - \vec{v}_2 + \vec{v}_3 - \vec{v}_4\right),$$

where the coefficient $a = \frac{Q}{4}\rho C\sqrt{A}$ and Q is a given constant.

Finally, the pressure is updated by the equation of state (i.e., the Mie-Grüneisen model in this paper):

$$p^{*n+1} = p(\rho^{*n+1}, e^{*n+1}).$$

4.2. Corrector step. In the corrector step, the physical variables are updated, similarly to the process in the predictor step as follows.

$$a_p^{n+1} = \tfrac{1}{M_p^{*n+1}} \sum_z \left(\vec{f}_z^p\right)^{*n+1} = \tfrac{1}{M_p^{*n+1}} \sum_z \left(\sigma_z \cdot \vec{C}_z^p + \vec{f}_{hgs}\right)^{*n+1}. \tag{20}$$

$$\vec{v}_p^{n+1} = \vec{v}_p^n + a_p^{n+1}\Delta t, \tag{21}$$

$$\vec{v}_p^{n+1/2} = \frac{1}{2}\left(\vec{v}_p^n + \vec{v}_p^{n+1}\right) = \vec{v}_p^n + \tfrac{\Delta t}{2} a_p^{n+1}. \tag{22}$$

$$e_z^{n+1} = e_z^n - \frac{\Delta t}{M_z^{*n+1}} \sum_p \left(\sigma_z \cdot \vec{C}_p^z + \vec{f}_{hgs}\right)^{*n+1} \cdot \vec{v}_p^{n+\frac{1}{2}}. \tag{23}$$

The discretized evolutionary equations of deviatoric stresses S_{rr}^{*n+1}, S_{zz}^{*n+1}, S_{rz}^{*n+1} read as follows.

$$S_{rz}^{n+1} = S_{rz}^{n} - \frac{\Delta t}{V_z^{*n+1}} \sum_p (\mathbf{N}_{rz} \cdot \vec{C}_p^z)^{*n+1} \cdot \vec{v}_p^{n+1/2}.$$

The pressure in the corrector step is updated again by the equation of state:

$$p^{n+1} = p(\rho^{n+1}, e^{n+1}).$$

The above predictor-corrector process makes the current scheme FCSLAEP the second-order accuracy. Moreover, the conservation of total energy still holds.

5. Numerical tests. In this section, we present a number of numerical examples of both elastic-plastic and hydrodynamic flows to validate the proposed FCSLAEP.

5.1. Sod's shock tube problem. (Hydrodynamic flow with the exact solution) The exact solution of this problem can assess the convergence and accuracy of FCSLAEP for the hydrodynamic flow simulation. For this problem, the computation domain is $[0, 1] \times [0, 0.1]$. In order to test the convergence, we compute this problem with 100×5, 200×5, and 400×5, 600×5, and 800×5 cells, respectively. The CFL number is taken to be 0.15 and the end time is $t = 0.1$. The computed pressure and density with different cells are shown in Fig. 2, from which we clearly see that the numerical solution converges to the exact solution.

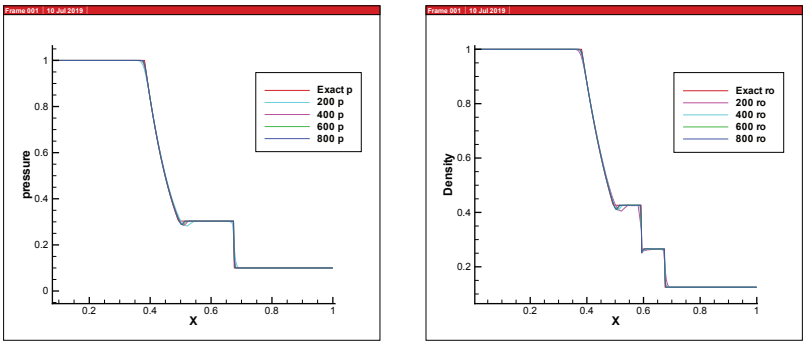

FIG. 2. *Sod's shock tube problem: Pressure and Density at t=0.1.*

5.2. Volume detonation. (Compare with the LS-DYNA code) This example assesses the conservation of total energy, where our FCSLAEP works as a simple formulation for hydrodynamics. For this problem we take the initial data as $\rho_0 = 1.712 g/cm^3$, the C-J detonation velocity is taken to be $D_J = 7.98 cm/us$ and the pressure to be $P_J = 29.5 Gpa$, $A = 5.242$, $B = 0.07678$, $R_1 = 4.2$, $R_2 = 1.1$, $w = 0.34$, $Q = 8.5 KJ/cm^3$. The computational domain is $(z, r) \in [0.0, 1.0] \times [0.0, 0.1]$. The grid is 200×5, and CFL number is taken to be 0.1. The computed pressure values at different time are listed in the left Fig. 3, while the values of total energy are given in the right Fig. 3.

From Fig. 3 one clearly observes that the detonation wave computed by FCSLAEP resolves better than that by the LS-DYNA code where a staggered compatible Lagrangian algorithm is also implemented. Moreover, the total energy computed by FCSLAEP is conserved up to machine precision, and appears like a straight line. while the total energy computed by the LS-DYNA code is not conserved and seems decreasing with time.

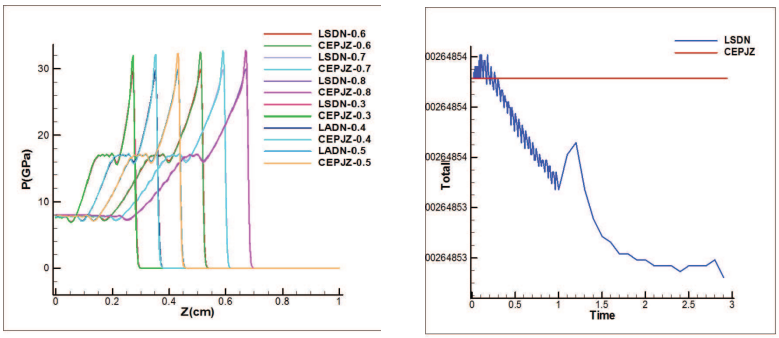

FIG. 3. *Volume detonation test: Pressure comparison between FCSLAEP and the LS-DYNA code, Total energy at T=0.3.*

5.3. Accuracy test. This test problem is taken from the papers [14, 20, 21] and has a smooth manufactured solution. Thus, we can use this problem to test the convergence order of the current scheme for smooth solutions. For the problem setting, we refer to [14, 20, 21] for the details. In the simulation, the physical constants/parameters are listed below: $a = 10000m/s$, $s_1 = 60 \times 10^6 Pa$, the constant internal energy $e_0 = 10^{-14}$, $\rho_0 = 8930kg/m^3$. The constants in EOS (6) are $a_0 = 3940m/s$, $\Gamma_0 = 2, s = 1.49$, the shear module $\mu = 45 \times 10^9 Pa$, the yielding strength $Y^0 = 90 \times 10^9 Pa$. The computational domain is $[0, 1] \times [0, 1]$ and the end time is taken to be $t = 1$. The periodic boundary condition is imposed, and the initial data are

$$\begin{gathered}\rho = \rho_0 \{1 - 0.1\sin(2\pi z) - 0.1\cos(2\pi r)\} \\ u = v = a, \quad e = e_0, \\ s_{zz} = s_1(\cos(2\pi z) - \sin(2\pi r)), \\ s_{rr} = -s_1(\sin(2\pi z) - \cos(2\pi r)), s_{zr} = s_{zz} + s_{rr}.\end{gathered}$$

With the above constants/parameters, the system (3)–(5) has a smooth manufactured solution in the form of

$$\begin{gathered}\rho = \rho_0 \{1 - 0.1 * sin\,[2\pi(z - at)] - 0.1cos\,[2\pi(r - bt)]\}, \\ u = v = a, \quad e = e_0, \\ s_{zz} = s_1(\cos(2\pi(z - at)) - \sin(2\pi(r - bt))), \\ s_{rr} = -s_1(\sin(2\pi(z - at)) - \cos(2\pi(r - bt))), s_{zr} = s_{zz} + s_{rr}.\end{gathered}$$

The errors in the L_2-norm between the computed solution by FCSLAEP and the manufactured solution are listed in Table 1, from which one sees that FCSLAEP achieves nearly the second-order accuracy. Moreover, the convergence order tends to the 2nd one as grids are refined.

5.4. Elastic-plastic piston-like problem. (Elastic-plastic flow with the exact solution) This test problem assesses the accuracy and convergence of FCSLAEP in simulating an elastic-plastic piston-like problem of copper with the Mie-Grneisen equation. This is a one-dimensional flow characterized by an analytical solution with a moving stress shock in a piece of copper. For a piston-like problem, being given the piston velocity, it is straightforward to solve the Riemann problem. The initial data of the elastic-plastic piston-like problem, which are the same as in [13], are characterized by: $\rho_0 = 8390kg/m^3$, $a_0 = 3940m/s$, $\Gamma_0 = 2$ and $s = 1.49$. The incremental elastic-plastic constitutive law is characterized by the shear modulus $\mu = 45 \times 10^9 Pa$, and

TABLE 1
Errors in L_2-norm between the numerical and manufactured solutions

N	ρ	Order	s_{zz}	Order
20	6.81236E-04		6.98149E-05	
40	2.01365E-04	1.75834	2.21403E-05	1.65686
80	5.68793E-05	1.82384	6.56841E-06	1.75306
160	1.41352E-05	2.00861	1.64194E-06	2.00014

the yield strength $Y_0 = 90 \times 10^6 Pa$. The computational domain is defined in polar coordinates by $(z, r) \in [0, 1] \times [0, 0.1]$, with 100×5, 200×5, 400×5, 600×5, 800×5, 1000×5 cells.

The initial pressure is $1 \times 10^5 Pa$ and the initial velocity is zero. The left boundary is a piston boundary with velocity $v_{left} = 20m/s$, whereas on the right, upper and down boundaries of the computational domain, the wall boundary conditions are imposed. The CFL number is taken to be 0.1 and the end time of the computation is $t_{end} = 150 \times 10^{-6} s$.

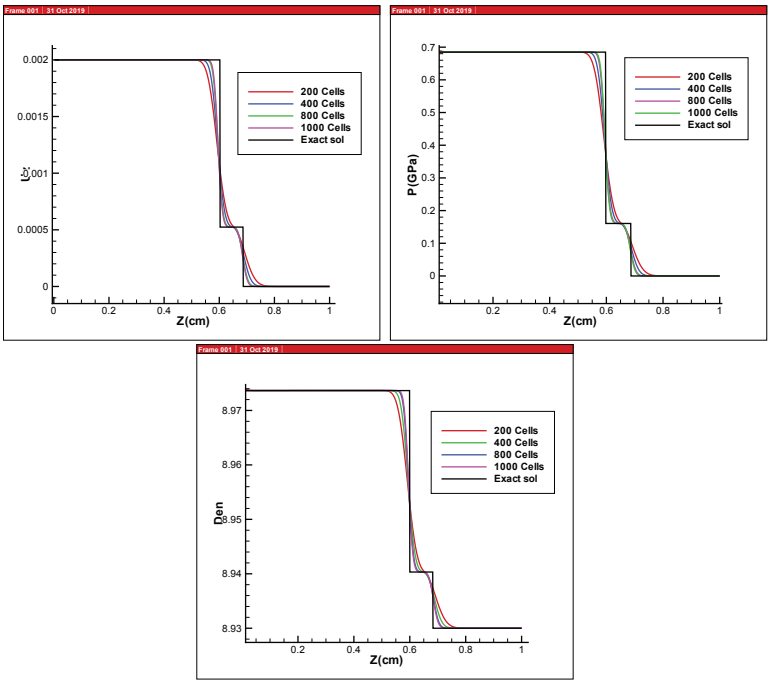

FIG. 4. *Piston-like problem: Velocity, Pressure and Density.*

The numerical results with different Δx are presented in Fig. 4 with the velocity (Left), pressure (Middle) and density (Right) at the end time. From Fig. 4 one can see that the numerical solution is converging to the exact solution in terms of the values and shock locations. The leading elastic shock wave and the followed plastic shock wave are well captured. Besides, there are no numerical oscillations near the shock waves.

5.5. Collapse of a thick-walled cylindrical Beryllium shell. (Elastic-plastic flow) This test problem was initially proposed by Howell and Ball in [2] to compute the collapse of a cylindrical beryllium shell. The initial inner and outer radii of the shell are $R_i = 80 \times 10^{-3}m$ and $R_0 = 100 \times 10^{-3}m$, respectively. The angle range of the computational field is $[0, \frac{\pi}{2}]$. The initial pressure is taken to be $p_0 = 10^5\ Pa$. This problem consists in computing the collapse of a cylindrical beryllium shell undergoing an initial radial velocity field directed towards its center. The initial velocity is towards the center of the shell and the initial radial velocity field is $-V_0\frac{R_i}{r}$, where V_0 is 417.1 m/s and $r = \sqrt{x^2 + y^2}$ is the radius.

The equation of state is given by the Mie-Grüneisen model:

$$p(V,\varepsilon) = \frac{a_0^2(V_0 - V)}{[V_0 - s(V_0 - V)]^2} + \frac{\Gamma(V)}{V}\left[\varepsilon - \frac{1}{2}\left(\frac{a_0(V_0 - V)}{V_0 - s(V_0 - V)}\right)^2\right] \tag{24}$$

with $\rho_0 = 1845kg/m^3$, $a_0 = 12870m/s$, $\Gamma_0 = 2$ and $s = 1.124$.

The initial kinetic energy of the shell is entirely converted into internal energy through plastic dissipation. The final state of the shell at the end of collapse is characterized by its inner and outer stopping radii which can be expressed analytically in terms of the initial condition. The incremental elastic-plastic constitutive law is characterized by the shear modulus $\mu = 151.9 \times 10^9 Pa$, and the yield strength $Y_0 = 330 \times 10^6 Pa$. In this problem, on the left and right boundaries the reflected boundary condition is imposed, while on the upper and down boundaries the free boundary condition is implemented. For this problem, Maire et al. in [13] pointed out that the analytic solution proposed by Howell and Ball in [2] is also suitable for this problem with a different EOS.

The computed density and pressure by FCSLAEP at the end time $t_{end} = 130 \times 10^{-6}s$ are given in Fig. 5, where three grids 20×16, 40×32 and 80×64 are used in order to demonstrate the convergence of the current scheme.

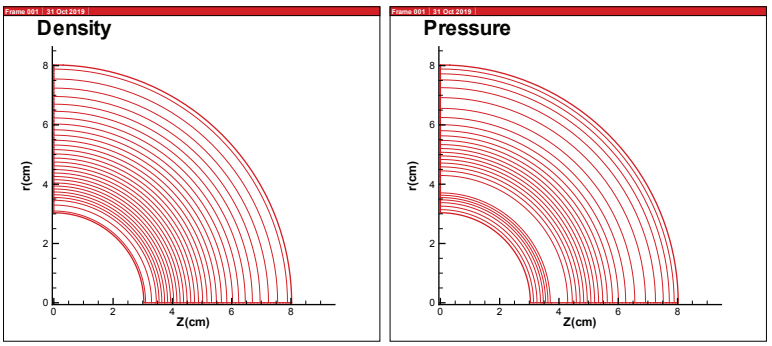

FIG. 5. *Collapse problem: Density and Pressure*

From Fig. 6 we see that the inner and outer stopping radii of the shell agree well with the theoretical values, and the numerical solution is converging to the analytical one. This shows that the current scheme seems to be convergent. From Fig. 6 one can also observe that the changes of the inner and outer radii of the shell with time are in good agreement with those of the analytical solution. This shows that FCSLAEP seems to be symmetric.

The errors between the asymmetric (inner/outer) radius and the average (inner/outer) radius are given in Fig. 7, from which we see that the computed density

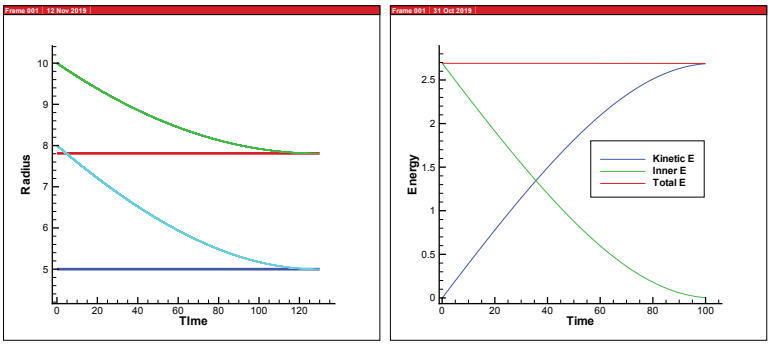

FIG. 6. *Collapse problem: Stopping radii and energies.*

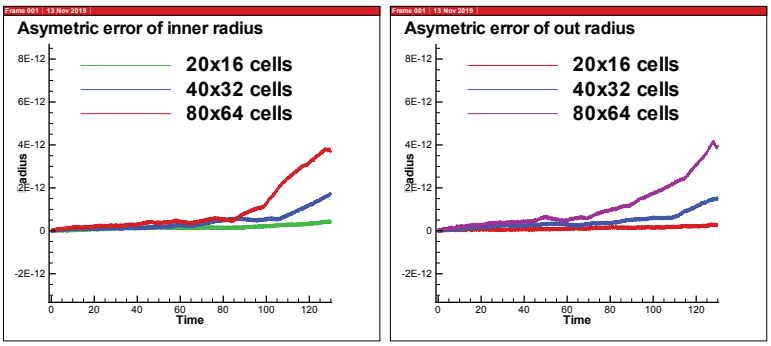

FIG. 7. *Collapse problem: Asymmetric errors of the (inner/outer) radius.*

and pressure seem symmetric, and moreover, the asymmetric errors are smaller than 1.0×10^{-12}.

6. Conclusions. In this paper, a fully compatible staggered Lagrangian algorithm is constructed for the system of two-dimensional elastic-plastic flows with Wilkins's constitutive model. The basic idea in the construction is that all governing equations of elastic-plastic flows, including the equations of deviatoric stress, are formulated into the form of the divergence and the gradient operators. Then, this hyperbolic system is discretized by adapting the method of support operators as well as an identity of operators, which has been employed to derive compatible sets of the fundamental vector differential operators in the discrete form. Compared with [15], the presence of the equations of deviatoric stress makes compatible discretization more complicated, and the main differences in the discretization lie in the following: As is well-known, the gradient operator acts on the pressure p in hydrodynamic flows, while for elastic-plastic flows in the staggered case, it is the divergence (but not the gradient) operator that acts on the zone centered strain tensor (but not on the pressure p) to produce a vector function at corners, which gives the temporal variation of the velocity. The divergence operator also acts on the velocity to produce a scalar function centered in a zone to model the temporal change of the volume and the deformation tensor. Contrary to hydrodynamic flows, the gradient operator in elastic-plastic flows acts on the velocity (but not on the pressure p) to produce a deformation tensor that includes the diliational shear, and rotational components, and models the temporal variation of the internal energy. Moreover, the (compatible) discretization of

the equations of deviatoric stress, which plays an important role in conserving the total energy and preserving the symmetry of solutions, exploits the ideas of replacing the finite volume surface integrals with the line integrals and rewriting the equations in the form with the internal energy on the right-hand side, so that one can use the gradient operator on the velocity in the discrete form. Consequently, this makes the current scheme FCSLAEP conserve the total energy and preserve the symmetry. We have presented a number of numerical tests, which demonstrate the robustness and convergence, the conservation of total energy and preservation of symmetry of FCSLAEP.

Acknowledgments. The research of Jiang was supported by National Key R&D Program (2020YFA0712200), National Key Project (GJXM92579), and NSFC (Grant No. 11631008, No. 12072043), the Sino-German Science Center (Grant No. GZ 1465) and the ISF-NSFC joint research program (Grant No. 11761141008).

REFERENCES

[1] M. L. Wilkins, *Methods in computational physics*, Volume 3, Chapter Calculation of elastic-plastic flow, Academic Press, 1964, pp. 211–263.

[2] B. P. Howell and G. J. Ball, *A free-Lagrange augmented Godunov method for the simulation of elastic-plastic solids*, J. Comput. Phys., 175 (2002), pp. 128–167.

[3] R. W. Anderson, V. A. Dobrev, T. V. Kolev, and R. N. Rieben, *Research paper presented at multimat2013 multi-material hydrodynamics simulations: monotonicity in high-order curvilinear finite elements arbitrary Lagrangian-Eulerian remap*, J. Numer. Mech. Fluids, 77 (2015), pp. 249–273.

[4] V. A. Dobrev, T. V. Kolev, R. N. Rieben, and V. Z. Tomov, *Multi-material closure model for high-order finite elements Lagrangian hydrodynamics*, J. Numer. Mech. Fluids, 82 (2016), pp. 689–706.

[5] R. W. Anderson, V. A. Dobrev, T. V. Kolev, and R. N. Rieben, *High-order multi-material ALE hydrodynamics*, SIAM J. Sci. Commput. 40:1 (2018), pp. B32–B35.

[6] R. N. Rieben and K. Weiss, *The multiphysics on advanced paltform project*, LLNL-TR-815869, 2020/10/21.

[7] V. A. Dobrev, T. V. Kolev, and R. N. Rieben, *Curvilinear finite elements for Lagrangian Hdynamics*, J. Numer. Mech. Fluids, 82 (2010), pp. 689–706.

[8] V. A. Dobrev, T. V. Kolev, and R. N. Rieben, *High order curvilinear finite elements for Lagrangian Hdynamics*, SIAM J. Sci. Comput., 34:5 (2012), pp. B606–B641.

[9] V. A. Dobrev, T. E. Ellis, T. V. Kolev, and R. N. Rieben, *High order curvilinear finite elements for axisymmetric Lagrangian hydrodynamics*, Computers & Fluids, 83 (2013), pp. 58–69.

[10] A. Johnen, J. F. Remacle, and C. Geuzaine, *Geometrical validity of curvilinear finite elements*, J. Comput. Physics., 223 (2013), pp. 359–372.

[11] V. A. Dobrev, T. V. Kolev, and R. N. Rieben, *High order curvilinear finite elements for elastic-plastic Lagrangian dynamics*, J. Comput. Physics., 237 (2014), pp. 1062–1080.

[12] V. A. Dobrev and R. N. Rieben, *A Tensor artificial viscosity using a finite element approach*, J. Comput. Physics., 228 (2009), pp. 8336–8366.

[13] P.-H. Maire, R. Abgrall, J. Breil, R. Loubère, and B. Rebourcet, *A nominally second-order cell-centered Lagrangian scheme for simulating elastic-plastic flows on two-dimensional unstructured grids*, J. Comput. Physics., 235 (2013), pp. 626–665.

[14] J. Cheng, Y. Jia, S. Jiang, and M. Yu, *A second order cell-centered Lagrangian method for 2D elastic-plastic flows*, Commun. in Comput. Phys., 22 (2017), pp. 1224–1257.

[15] E. J. Caramana, D. Burton, M. J. Shashkov, and P. P. Whalen, *The Construction of Compatible Hydrodynamics Algorithm Utilizing Conservation of Total Energy*, J. Comput. Phys., 146 (1998), pp. 227–262.

[16] A. Barlow, R. Hill, and M. Shashkov, *Constrained optimization framework for interface-aware sun-scale dynamics closure models for multimaterial cells in Lagrangian and arbitrary Lagtangian-Eulerican hydrodynamics*, J. Comput. Phys., 146 (2014), pp. 227–262.

[17] Z. Lin, Z. H.,and R. L. Wang, *Compatible Hydrodynamics Algorithms and Their Applications*, GF report, 2006-05-30, 2006.

[18] H. B. Zhou, J. Xiong, Y. Y. Wu, W. T. Liu, S. D. Zhang, etc, *The artificial viscidity in tensor form and its application in Compatible Hydrodynamics Algorithm*, T04-ZJJE-08, 2004.

[19] D. E. Burton, *Multidimensional Discretization of Conservation Laws for Unstructured Polyhedral Grids*, Technical Report UCRL-JC-118306, Lawrence Livermore National Laboratory, 1994.

[20] P. J. Roache, *Code verification by the method of manufactured solutions*, Trans. ASME. J. Fluids Engineering, 124 (2002), pp. 4–10.

[21] K. Salari and P. Knupp, *Code verification by the method of manufactured solutions*, Sandia Report, Sandia National Laboratories, SAND2000-1444, 2000.